GEOLOGY | THE GEOLOGICAL SOCIETY OF AMERICA®

Can nanolites enhance eruption explosivity?

Francisco Cáceres[1]*, Fabian B. Wadsworth[2,3], Bettina Scheu[1], Mathieu Colombier[1], Claudio Madonna[4], Corrado Cimarelli[1], Kai-Uwe Hess[1], Melanie Kaliwoda[5], Bernhard Ruthensteiner[6] and Donald B. Dingwell[1]

[1]Department of Earth and Environmental Sciences, Ludwig-Maximilians-Universität, Theresienstrasse 41, 80333 Munich, Germany
[2]Department of Earth Sciences, Durham University, Durham DH1 4LY, UK
[3]Centre for Advanced Studies, Ludwig-Maximilians-Universität, 80802 Munich, Germany
[4]Department of Earth Sciences, ETH Zürich, 8092 Zurich, Switzerland
[5]Mineralogical State Collection Munich (SNSB), Munich, Germany
[6]Zoologische Staatssammlung, 80333 Munich, Germany

ABSTRACT

Degassing dynamics play a crucial role in controlling the explosivity of magma at erupting volcanoes. Degassing of magmatic water typically involves bubble nucleation and growth, which drive magma ascent. Crystals suspended in magma may influence both nucleation and growth of bubbles. Micron- to centimeter-sized crystals can cause heterogeneous bubble nucleation and facilitate bubble coalescence. Nanometer-scale crystalline phases, so-called "nanolites", are an underreported phenomenon in erupting magma and could exert a primary control on the eruptive style of silicic volcanoes. Yet the influence of nanolites on degassing processes remains wholly uninvestigated. In order to test the influence of nanolites on bubble nucleation and growth dynamics, we use an experimental approach to document how nanolites can increase the bubble number density and affect growth kinetics in a degassing nanolite-bearing silicic magma. We then examine a compilation of these values from natural volcanic rocks from explosive eruptions leading to the inference that some very high naturally occurring bubble number densities could be associated with the presence of magmatic nanolites. Finally, using a numerical magma ascent model, we show that for reasonable starting conditions for silicic eruptions, an increase in the resulting bubble number density associated with nanolites could push an eruption that would otherwise be effusive into the conditions required for explosive behavior.

INTRODUCTION

A key question faced by volcanologists is whether the ascent of magma in the shallow crust will result in an explosive eruption of ash and gas or a potentially less-dangerous effusive eruption of lava. Indeed, these styles of eruption can switch during a single eruption (e.g., Rust and Cashman, 2004; Colombier et al., 2017a; Cassidy et al., 2018). Magma ascent is driven by bubble growth, and a first-order control on whether an eruption will be explosive or not is the rate at which bubbles grow in the melt (e.g., McBirney and Murase, 1970; Forte and Castro, 2019) and the propensity for permeable outgassing during bubble growth (e.g., Degruyter et al., 2012). Both of these factors—bubble growth rates and permeable outgassing efficiency—are influenced strongly by the number density of bubbles that form in nucleation events, because

high bubble number densities shorten the distances for water to diffuse between bubbles, reduce the viscous resistance to growth, and result in smaller bubble-bubble pairs at the onset of permeability (e.g., Gonnermann and Manga, 2007; Degruyter et al., 2012).

Bubble number densities are dominantly controlled by the local decompression rate, volatile diffusivity, volatile concentration, temperature, and surface tension (e.g., Toramaru, 2006; Shea, 2017). Crystals, especially those at micron to millimeter scale, impart the magma with a distributed internal interface to serve as a surface for heterogeneous nucleation, reducing the supersaturation conditions needed to nucleate bubbles (Hurwitz and Navon, 1994; Mangan et al., 2004; Gardner and Denis, 2004; Cluzel et al., 2008; Larsen, 2008; Shea, 2017; Pleše et al., 2018) and to facilitate bubble coalescence (e.g., Lindoo et al., 2017). In turn, crystals "stiffen" the viscous response of the magma such

that bulk expansion of the bubbles is resisted (Oppenheimer et al., 2015). Thus, the observation that nanolites, or nanometer-scale crystalline phases, are extant in products of explosive volcanism raises the general question as to what their physical role might be in bubble dynamics during magma ascent.

Nanolites have been identified in both natural volcanic products (e.g., Sharp et al., 1996; Mujin and Nakamura, 2014; Barone et al., 2016; Zellmer et al., 2016; Colombier et al., 2017b) and experimental products (e.g., Liebske et al., 2003; Di Muro et al., 2006; Di Genova et al., 2017). They are inferred to crystallize in magmas at low pressure (Mujin and Nakamura, 2014) and during slow cooling (Liebske et al., 2003; Di Muro et al., 2006). The formation of nanolites has been suggested to favor heterogeneous bubble nucleation (e.g., Shea, 2017), and they have been invoked as a potential control on the eruptive style of volcanoes (Mujin and Nakamura, 2014; Mujin et al., 2017; Di Genova et al., 2017). However, the mechanism behind this control on the eruptive style remains unclear. Here, we present results of experiments designed to explore the degassing dynamics of rhyolitic magma with and without nanolites, and we find that the presence of nanolites can amplify bubble number densities by many orders of magnitude. We use this finding to argue that nanolites may be capable of inducing explosivity in otherwise effusive eruptions.

MATERIALS AND EXPERIMENTAL METHODS

We used two volcanic materials to conduct our bubble-growth experiments: (1) a natural iron-rich nanolite-free rhyolite obsidian (Fig. 1A) with 0.15 wt% dissolved H_2O,

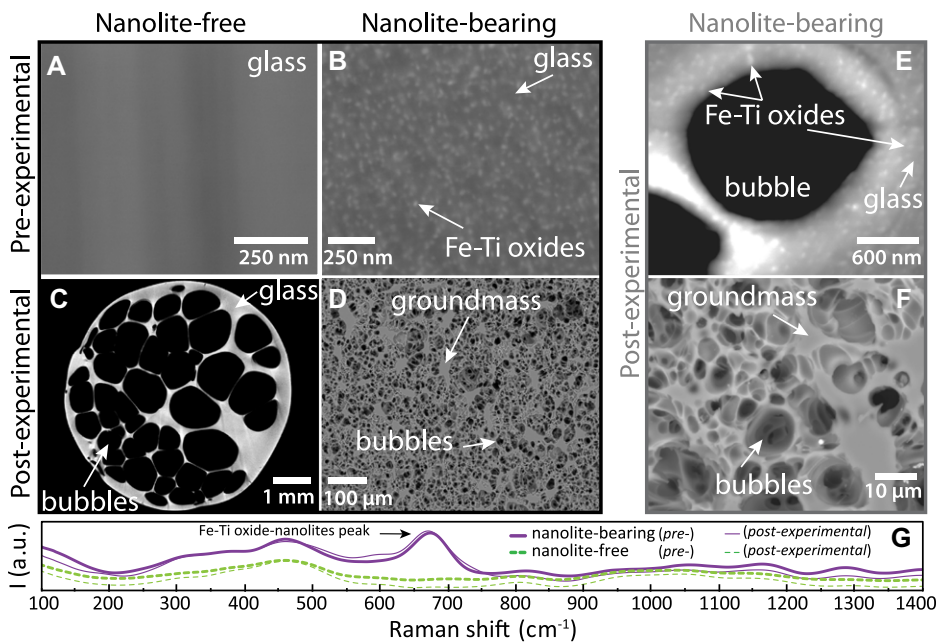*E-mail: francisco.caceres@min.uni-muenchen.de

Figure 1. Pre- and post-experimental samples. (A) Backscattered electron–scanning electron microscope (BSE-SEM) image of nanolite-free glass. (B) BSE-SEM image of nanolite-bearing sample with nanolite number density N_n of ~10^{12} mm^{-3}. (C) X-ray computed tomography image of post-experimental nanolite-free sample with ~60 vol% vesicularity and bubble number density N_b of ~10^0 mm^{-3}. (D) BSE-SEM image of post-experimental nanolite-bearing sample with ~70 vol% vesicularity and N_b of ~10^7 mm^{-3}. (E) Zoom image of a post-experimental nanolite-bearing sample and nanolite-bubble coexistence. (F) Zoom image of bubbles and interstitial groundmass (nanolites + glass) in a post-experimental nanolite-bearing sample showing bubble interaction and sizes. (G) Raman spectra for samples pre- and post-experiment. Fe-Ti oxide nanolites peak (~670 cm^{-1}) is indicated by the arrow. I—intensity; a.u.—arbitrary units.

and (2) a synthesized nanolite-bearing sample (Fig. 1B) of the same rhyolitic composition with 0.32 wt% dissolved H_2O (see the Supplemental Material[1]). To form nanolites, we re-sintered a powder of the natural obsidian in a sealed container with a small amount of water in a hot isostatic press at 800°C and 23 MPa. Nanolites are ubiquitous in the synthesized sample, with an average nanolite number density N_n of ~3.5×10^{12} mm^{-3} and an average size of 10–50 nm, corresponding to ~2 vol% of the magma. The crystals and bubbles were investigated via backscattered electron images (Fig. 1) of polished samples using a Hitachi SU5000 scanning electron microscope. A confocal Raman spectrometer was used to identify nanolites (see the Supplemental Material). The nanolites in the groundmass of the synthesized sample correspond to Fe-Ti oxides based on a peak in Raman spectra at 670–690 cm^{-1}. The same peak is absent from the spectra of the glass in the natural obsidian, confirming the absence of Fe-Ti oxide nanolites (Fig. 1G).

We heated these two sample types in an optical dilatometer at 1–60°C min^{-1} to isothermal dwells at 820–1000°C. We recorded their real-time sample volume and shape as they crossed the glass transition, followed by rapid expansion (see the Supplemental Material). The experimental products for the two sample types were then compared.

EXPERIMENTAL OBSERVATIONS

When heated at the same heating rates, the nanolite-bearing sample always began expanding significantly earlier and with a higher expansion rate than the nanolite-free sample (Fig. 2). While the two sample types (nanolite-free and nanolite-bearing) had subtly different initial water concentrations (0.15 versus 0.32 wt%),
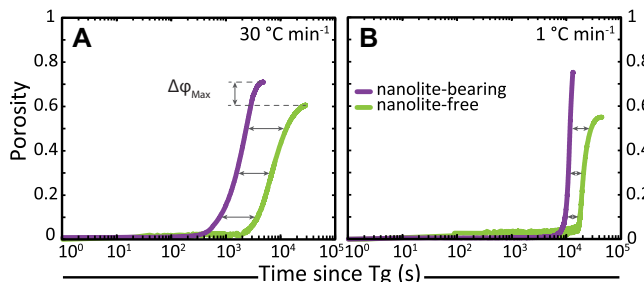
we assume that the discrepancy in onset time and expansion rate (bubble growth) cannot be attributed to this small difference in starting water content. We note that even when comparing conditions where the calculated melt viscosity is higher and water diffusivity is lower in the nanolite-bearing sample (Fig. 2), the growth rate in the nanolite-bearing samples were higher. Thus, this gap between the two sample types is attributed to the difference in their nucleated bubble number density.

Using run products for experiments that reached equilibrium porosity and bubble size, we determined that for the natural obsidian, the bubble number density (N_b) produced during the experiments was $10^{-1} \le N_b \le 10^1$ mm^{-3} and final bubble sizes (bubble diameter, R_d) were $0.2 \le R_d \le 1.5$ mm (Fig. 1C), while for the re-melted, nanolite-bearing sample, N_b was much higher, at $10^6 \le N_b \le 10^7$ mm^{-3}, with significantly smaller final bubble sizes of $10^{-3} \le R_d \le 10^{-1}$ mm (Fig. 1D). The values obtained here for the natural, nanolite-free obsidian are consistent with experiments carried out with same composition and at similar conditions (Ryan et al., 2015).

DISCUSSION

The number density of homogeneously nucleated bubbles during degassing of an ascending magma is dominantly controlled by the decompression rate (e.g., Toramaru, 2006; Shea, 2017). However, heterogeneous nucleation may decrease the decompression rate needed to produce the same N_b by orders of magnitude (e.g., Cluzel et al., 2008; Hamada et al., 2010; Shea, 2017). High N_b (~10^7 mm^{-3}) in natural silicic explosive products (e.g., the 7.7 ka Mount Mazama eruption, Oregon, USA; Klug et al., 2002) have been attributed to a combination of fast decompression rates and the presence of relatively high (10^0–10^2 mm^{-3}) crystal number densities during degassing (e.g., Hamada et al., 2010), with an emphasis on the additional role played by decompression (or ascent) rates. Our data suggest that the nucleation of nanolites in magmas could result in high bubble number

Figure 2. Experimental porosity evolution for nanolite-free (green) and nanolite-bearing (purple) samples at 30 °C min^{-1} (A) and 1 °C min^{-1} (B) heating rates. Nanolite-free samples were heated up to 1000 °C (glass viscosity η ~ 10^7 Pa·s, water diffusivity D ~ 6×10^{-13} m^2 s^{-1}) and nanolite-bearing samples were heated up to 820 °C (η ~ 10^9 Pa·s, D ~ 2×10^{-13} m^2 s^{-1}); η and D were calculated using the models of Hess and Dingwell (1996) and Zhang and Ni (2010) with Liu et al. (2005) for melt-water concentration. The time difference when sample pairs reached 0.1, 0.3, and 0.5 porosity values is shown as reference (gray arrows), as well as the difference in maximum porosity. Tg—glass transition temperature.
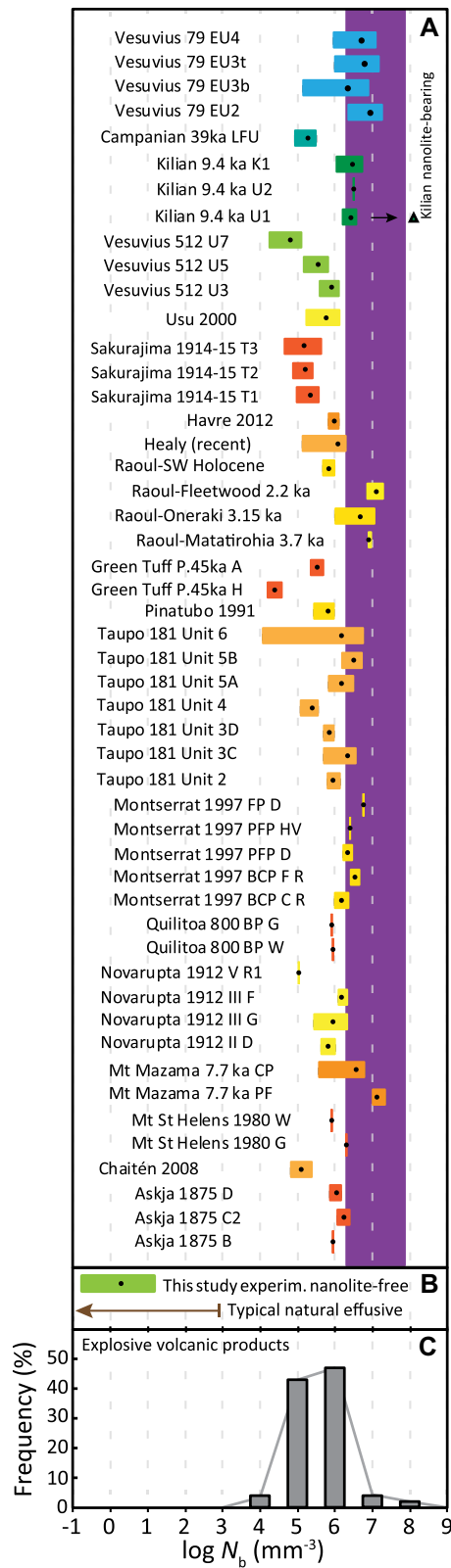
Figure 3. Bubble number density, N_b, of products of volcanic eruptions. (A) N_b recorded in clasts from different phases or units in explosive eruptions with minimum and maximum reported values; black dots indicate mean values. Colors denote glass composition: orange and yellow for rhyolitic, green for trachytic, and blue for phonolitic. Purple region shows the experimental range for nanolite-rich samples in this study. For Kilian U1, the black triangle shows the value with nanolites. (B) Range of N_b for nanolite-free experimental samples in this study (green) and referential range for typical varied natural effusive products. (C) Frequency distribution of N_b mean values for which >80% of data fall in the range of 10^5–10^6 mm^{-3}. See the Supplemental Material (see footnote 1) for references.

To put our results in context, we compiled published estimates of N_b in natural products of explosive eruptions with a range of magmatic compositions (Fig. 3A). These data show that across the range from intermediate to silicic magmas, mean N_b tend to be ~10^5–10^6 mm^{-3}, with maxima at >10^8 mm^{-3} (Fig. 3C; similar to data compiled by Shea [2017]). We note that the bubble number densities produced in our nanolite-bearing samples are in the higher end of the range of bubble number densities (≥10^6 mm^{-3}) found in natural explosive products. For comparison, data for N_b in intermediate to silicic effusive eruptions are sparse, but typical values are <10^3 mm^{-3} (Fig. 3B).

Nanolites are not widely reported in erupted products, and therefore the subset of this compilation for which nanolites have been identified is low. Fe-Ti-oxide nanolites have been observed in tephra from Kilian volcano, France

(Colombier et al., 2017b; see the Supplemental Material). These nanolite-bearing products have N_b as much as two orders of magnitude higher than the nanolite-free products of the same eruption (Fig. 3A). In the case of the 2011 Shinmoedake eruption, Japan (Mujin and Nakamura, 2014; Mujin et al., 2017), nanolites of low-Ca pyroxenes, plagioclase, and Fe-Ti oxides are present throughout the transition sequence from sub-Plinian to effusive eruptive style. Even though the nature of these nanolites differs from those in this study, due to the different composition of the magma involved, nanolites are present in the products of the first and most explosive phase of the eruption with N_n of ~10^{13} mm^{-3} comparable to those in this study (~10^{12} mm^{-3}).

This compilation of naturally occurring bubble number densities (Fig. 3) along with the few observations that exist for the natural occurrence of nanolites suggest that nanolites may play a role in increasing the bubble number density relative to nanolite-free magma. This is consistent with the findings of our experimental work (Figs. 1 and 3). While we do not claim that this is the only cause of high bubble number densities, we propose that this process can operate in shallow magma ascent.

APPLICATION TO SILICIC MAGMAS

Here, we have established that silicic magmas that form nanolites prior to bubble nucleation events can result in high bubble number densities compared with nanolite-free magmas. In a second step, we show that the high experimental N_b values in nanolite-bearing melts are at the upper end of naturally occurring ones, and
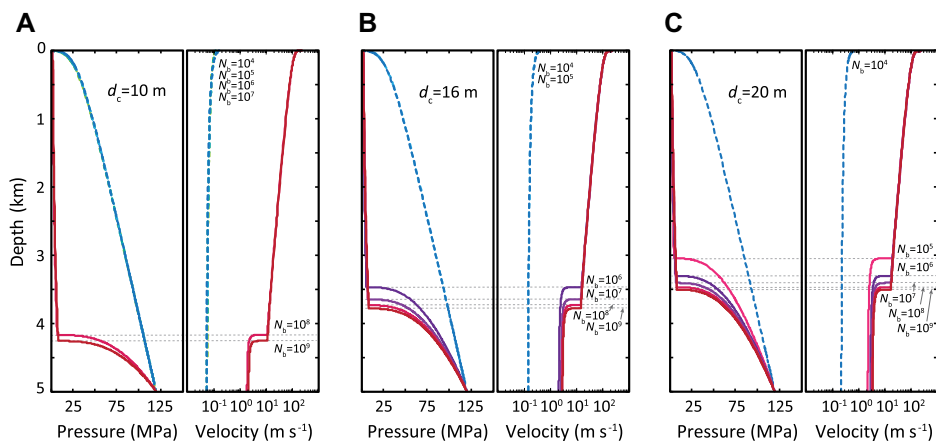

Figure 4. One-dimensional magma ascent model (Degruyter et al., 2012). We used a 5-km-long conduit and an initial reservoir pressure P_0 = 120 MPa, magma temperature T = 825 °C, initial water content C_0 = 4.27 wt%, and initial bubble size (radius) R_0 = 10^{-7} m, based on the 2008 Chaitén (Chile) eruption (Castro and Dingwell, 2009; see the Supplemental Material [see footnote 1]). Where not stated, we used default inputs from Degruyter et al. (2012). We systematically explored the effect of bubble number densities (N_b) in the range of 10^4–10^9 mm^{-3} on the evolution of the pressure gradient, ascent velocity, and initiation of fragmentation in a conduit of diameters (d_c) 10 m (A), 16 m (B), and 20 m (C). Note that fragmentation is indicated by a jump in pressure or velocity gradients, and is marked with gray dotted lines. Solid colored lines represent explosive ascent paths, and dashed colored lines represent effusive ascent paths. For a given conduit diameter, an increase in N_b can induce fragmentation.

densities and associated high bubble growth rates in situations where nanolites grow below or within the kinetic window of bubble nucleation. This implies a possibility of reaching high bubble number densities by heterogeneous nucleation of bubbles on nanolites even at relatively low decompression rates.

that in the few available cases, nanolites have been found in high-N_b products of explosive eruptions. As a final step, we employ a reference magma ascent model to show what the effect of such an increase in N_b may be in ascending magmas. In doing so, we do not aim to model heterogeneous nucleation of bubbles on nanolites explicitly, but rather use existing tools to build the case for the critical effect nanolites may have in an ascending magma.

We simulated magma ascent in a conduit using the one-dimensional two-phase model developed by Degruyter et al. (2012) that considers magma ascent and permeable outgassing at high porosities. Although this model works on the basis of equilibrium degassing and does not consider the mechanism (i.e., homogeneous or heterogeneous) and kinetics of bubble nucleation, it is suitable for investigating the effect that existing bubbles exert on the eruptive behavior of ascending magma in a volcanic conduit, because it predicts whether a magma will fragment during ascent or not, effectively showing whether an eruption could be effusive or explosive at the Earth's surface. This model requires an input of N_b and initial bubble size, as well as conditions regarding the conduit dimensions, initial magma storage depth, temperature, and initial water content. We used three different realistic conduit diameters (10, 16, and 20 m) and magma starting conditions, such as those of the well-studied case of the 2008 Chaitén (Chile; Castro and Dingwell, 2009) eruption (Fig. 4; see the Supplemental Material). We solved this model by varying N_b, using the same range found in natural explosive products and in our experiments (Fig. 3A).

The simulations (Fig. 4) show that for a given range of common conduit dimensions, the range of N_b found in natural magmas (10^4–10^8 mm^{-3}) can straddle effusive and explosive eruptive style. Although the conduit diameter plays a first-order role, we find that for a given geometry, the increase in N_b associated with bubble nucleation on nanolites could result in a transition from effusive to explosive eruption (Fig. 4). These results are also consistent with low and high N_b inferred for effusive and explosive eruptions respectively (e.g., Cluzel et al., 2008). Moreover, for the conduit diameters investigated, the range of N_b that appears to be associated with nanolites (Fig. 3) is sufficiently high to result in explosive volcanism in most of the studied scenarios.

CONCLUDING REMARKS

We conclude from our experiments that nanolites can be efficient sites for bubble nucleation leading to high bubble number densities and growth rates. We observe that high bubble number densities such as those produced by nanolite-bearing samples are found in natural explosive volcanic products. We use these obser-

vations and numerical model results to propose that nanolites may play a role in enhancing the propensity for eruptions to be explosive. The conditions of undercooling required for nanolite crystallization remain poorly understood, and further investigation is required to link the nanolite nucleation window with the vesiculation window for natural magma ascent conditions.

REFERENCES CITED

Barone, G., Mazzoleni, P., Corsaro, R.A., Costagliola, P., Di Benedetto, F., Ciliberto, E., Gimeno, D., Bongiorno, C., and Spinella, C., 2016, Nanoscale surface modification of Mt. Etna volcanic ashes: Geochimica et Cosmochimica Acta, v. 174, p. 70–84, https://doi.org/10.1016/j.gca.2015.11.011.

Cassidy, M., Manga, M., Cashman, K., and Bachmann, O., 2018, Controls on explosive-effusive volcanic eruption styles: Nature Communications, v. 9, 2839, https://doi.org/10.1038/s41467-018-05293-3.

Castro, J.M., and Dingwell, D.B., 2009, Rapid ascent of rhyolitic magma at Chaitén volcano, Chile: Nature, v. 461, p. 780–783, https://doi.org/10.1038/nature08458.

Cluzel, N., Laporte, D., Provost, A., and Kannewischer, I., 2008, Kinetics of heterogeneous bubble nucleation in rhyolitic melts: Implications for the number density of bubbles in volcanic conduits and for pumice textures: Contributions to Mineralogy and Petrology, v. 156, p. 745–763, https://doi.org/10.1007/s00410-008-0313-1.

Colombier, M., Wadsworth, F.B., Gurioli, L., Scheu, B., Kueppers, U., Di Muro, A., and Dingwell, D.B., 2017a, The evolution of pore connectivity in volcanic rocks: Earth and Planetary Science Letters, v. 462, p. 99–109, https://doi.org/10.1016/j.epsl.2017.01.011.

Colombier, M., Gurioli, L., Druitt, T.H., Shea, T., Boivin, P., Miallier, D., and Cluzel, N., 2017b, Textural evolution of magma during the 9.4-ka trachytic explosive eruption at Kilian Volcano, Chaîne des Puys, France: Bulletin of Volcanology, v. 79, 17, https://doi.org/10.1007/s00445-017-1099-7.

Degruyter, W., Bachmann, O., Burgisser, A., and Manga, M., 2012, The effects of outgassing on the transition between effusive and explosive silicic eruptions: Earth and Planetary Science Letters, v. 349–350, p. 161–170, https://doi.org/10.1016/j.epsl.2012.06.056.

Di Genova, D., Kolzenburg, S., Wiesmaier, S., Dallanave, E., Neuville, D.R., Hess, K.-U., and Dingwell, D.B., 2017, A compositional tipping point governing the mobilization and eruption style of rhyolitic magma: Nature, v. 552, p. 235–238, https://doi.org/10.1038/nature24488.

Di Muro, A., Villemant, B., Montagnac, G., Scaillet, B., and Reynard, B., 2006, Quantification of water content and speciation in natural silicic glasses (phonolite, dacite, rhyolite) by confocal microRaman spectrometry: Geochimica et Cosmochimica Acta, v. 70, p. 2868–2884, https://doi.org/10.1016/j.gca.2006.02.016.

Forte, P., and Castro, J.M., 2019, H$_2$O-content and temperature limit the explosive potential of rhyo-

lite magma during Plinian eruptions: Earth and Planetary Science Letters, v. 506, p. 157–167, https://doi.org/10.1016/j.epsl.2018.10.041.

Gardner, J.E., and Denis, M.-H., 2004, Heterogeneous bubble nucleation on Fe-Ti oxide crystals in high-silica rhyolitic melts: Geochimica et Cosmochimica Acta, v. 68, p. 3587–3597, https://doi.org/10.1016/j.gca.2004.02.021.

Gonnermann, H.M., and Manga, M., 2007, The fluid mechanics inside a volcano: Annual Review of Fluid Mechanics, v. 39, p. 321–356, https://doi.org/10.1146/annurev.fluid.39.050905.110207.

Hamada, M., Laporte, D., Cluzel, N., Koga, K.T., and Kawamoto, T., 2010, Simulating bubble number density of rhyolitic pumices from Plinian eruptions: Constraints from fast decompression experiments: Bulletin of Volcanology, v. 72, p. 735–746, https://doi.org/10.1007/s00445-010-0353-z.

Hess, K.-U., and Dingwell, D.B., 1996, Viscosities of hydrous leucogranitic melts: A non-Arrhenian model: American Mineralogist, v. 81, p. 1297–1300, https://doi.org/10.2138/am-1996-9-1031.

Hurwitz, S., and Navon, O., 1994, Bubble nucleation in rhyolitic melts: Experiments at high pressure, temperature, and water content: Earth and Planetary Science Letters, v. 122, p. 267–280, https://doi.org/10.1016/0012-821X(94)90001-9.

Klug, C., Cashman, K.V., and Bacon, C.R., 2002, Structure and physical characteristics of pumice from the climactic eruption of Mount Mazama (Crater Lake), Oregon: Bulletin of Volcanology, v. 64, p. 486–501, https://doi.org/10.1007/s00445-002-0230-5.

Larsen, J.F., 2008, Heterogeneous bubble nucleation and disequilibrium H$_2$O exsolution in Vesuvius K-phonolite melts: Journal of Volcanology and Geothermal Research, v. 175, p. 278–288, https://doi.org/10.1016/j.jvolgeores.2008.03.015.

Liebske, C., Beherens, H., Holtz, F., and Lange, R.A., 2003, The influence of pressure and composition on the viscosity of andesitic melts: Geochimica et Cosmochimica Acta, v. 67, p. 473–485, https://doi.org/10.1016/S0016-7037(02)01139-0.

Liu, Y., Zhang, Y., and Behrens, H., 2005, Solubility of H$_2$O in rhyolitic melts at low pressures and a new empirical model for mixed H$_2$O–CO$_2$ solubility in rhyolitic melts: Journal of Volcanology and Geothermal Research, v. 143, p. 219–235, https://doi.org/10.1016/j.jvolgeores.2004.09.019.

Mangan, M.T., Sisson, T.W., and Hankins, W.B., 2004, Decompression experiments identify kinetic controls on explosive silicic eruptions: Geophysical Research Letters, v. 31, L08605, https://doi.org/10.1029/2004GL019509.

McBirney, A.R., and Murase, T., 1970, Factors governing the formation of pyroclastic rocks: Bulletin Volcanologique, v. 34, p. 372–384, https://doi.org/10.1007/BF02596762.

Mujin, M., and Nakamura, M., 2014, A nanolite record of eruption style transition: Geology, v. 42, p. 611–614, https://doi.org/10.1130/G35553.1.

Mujin, M., Nakamura, M., and Miyake, A., 2017, Eruption style and crystal size distributions: Crystallization of groundmass nanolites in the 2011 Shinmoedake eruption: American Mineralogist, v. 102, p. 2367–2380, https://doi.org/10.2138/am-2017-6052CCBYNCND.

Oppenheimer, J., Rust, A.C., Cashman, K.V., and Sandnes, B., 2015, Gas migration regimes and outgassing in particle-rich suspensions: Frontiers in Physics, v. 3, 60, https://doi.org/10.3389/fphy.2015.00060.

Pleše, P., Higgins, M.D., Mancini, L., Lanzafame, G., Brun, F., Fife, J.L., Casselman, J., and Baker, D.R., 2018, Dynamic observations of vesiculation reveal the role of silicate crystals in bubble nucleation and growth in andesitic magmas: Lithos, v. 296–299, p. 532–546, https://doi.org/10.1016/j.lithos.2017.11.024.

Rust, A.C., and Cashman, K.V., 2004, Permeability of vesicular silicic magma: Inertial and hysteresis effects: Earth and Planetary Science Letters, v. 228, p. 93–107, https://doi.org/10.1016/j.epsl.2004.09.025.

Ryan, A.G., Russell, J.K., Hess, K.-U., Phillion, A.B., and Dingwell, D.B., 2015, Vesiculation in rhyolite at low H_2O contents: A thermodynamic model: Geochemistry Geophysics Geosystems, v. 16, p. 4292–4310, https://doi.org/10.1002/2015GC006024.

Sharp, T.G., Stevenson, R.J., and Dingwell, D.B., 1996, Microlites and "nanolites" in rhyolitic glass: Microstructural and chemical characterization: Bulletin of Volcanology, v. 57, p. 631–640, https://doi.org/10.1007/s004450050116.

Shea, T., 2017, Bubble nucleation in magmas: A dominantly heterogeneous process?: Journal of Volcanology and Geothermal Research, v. 343, p. 155–170, https://doi.org/10.1016/j.jvolgeores.2017.06.025.

Toramaru, A., 2006, BND (bubble number density) decompression rate meter for explosive volcanic eruptions: Journal of Volcanology and Geothermal Research, v. 154, p. 303–316, https://doi.org/10.1016/j.jvolgeores.2006.03.027.

Zellmer, G.F., Sakamoto, N., Hwang, S.-L., Matsuda, N., Iizuka, Y., Moebis, A., and Yurimoto, H., 2016, Inferring the effects of compositional boundary layers on crystal nucleation, growth textures, and mineral chemistry in natural volcanic tephras through submicron-resolution imaging: Frontiers in Earth Science, v. 4, 88, https://doi.org/10.3389/feart.2016.00088.

Zhang, Y., and Ni, H., 2010, Diffusion of H, C, and O components in silicate melts: Reviews in Mineralogy and Geochemistry, v. 72, p. 171–225, https://doi.org/10.2138/rmg.2010.72.5.